Journal Pre-proofs

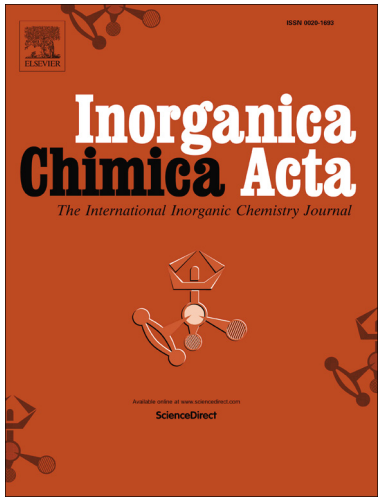

Research paper

Cytotoxicity and reactivity of a redox active 1,4-quinone-pyrazole compound and its Ru(II)-*p*-cymene complex

Kallol Purkait, Arindam Mukherjee

PII: S0020-1693(19)31110-7
DOI: https://doi.org/10.1016/j.ica.2019.119361
Reference: ICA 119361

To appear in: *Inorganica Chimica Acta*

Received Date: 30 July 2019
Revised Date: 13 November 2019
Accepted Date: 12 December 2019

Please cite this article as: K. Purkait, A. Mukherjee, Cytotoxicity and reactivity of a redox active 1,4-quinone-pyrazole compound and its Ru(II)-*p*-cymene complex, *Inorganica Chimica Acta* (2019), doi: https://doi.org/10.1016/j.ica.2019.119361

Cytotoxicity and reactivity of a redox active 1,4-quinone-pyrazole compound and its Ru(II)-*p*-cymene complex

Kallol Purkait and Arindam Mukherjee*[a]

[a]Department of Chemical Sciences, Indian Institute of Science Education and Research Kolkata, Nadia-741246, India.

*Corresponding author

Email: a.mukherjee@iiserkol.ac.in (A. Mukherjee)

Keywords: Ruthenium, *p*-cymene, quinone, hypoxia active, ROS.

This article is dedicated to Prof. G. K. Lahiri on the occasion of his 60th birthday.

Abstract: Quinone based compounds display activation in hypoxia, an environment prevalent in tumours. We have synthesized a bis(pyrazole) based 1,4-quinone compound suitable for metal chelation. The quinone (L2) converted to hydroquinone (H_2L1) during the complex synthesis leading to $[Ru^{II}(\eta^6\text{-}p\text{-cym})(H_2L1)Cl](PF_6)$ (**1**). We found from ^1H NMR studies that in the methanolic solution L2 stoichiometrically converted to H_2L1 while oxidizing the methanol to formaldehyde. L2 crystallized in monoclinic space group *I*2/a while complex **1** crystallizes in $P2_1/c$. Cyclic voltammetry of the redox non-innocent L2 showed quasi-reversible (ΔEp = 67 mV) redox behaviour with $E_{1/2}$ at 0.12 V w.r.t. NHE. Complex **1** is stable at pH 7.4 in presence of 4 mM chloride and does not hydrolyse even up to 24 h. L2 showed IC_{50} values of 155 and 123 μM against metastatic breast adenocarcinoma (MDA-MB-231) and pancreatic carcinoma (MIA PaCa-2) respectively. L2 gets activated by ca. 2.7-fold in hypoxia and prevents migration of MDA-MB-231 cells. The mechanistic studies showed ROS accumulation and oxidation of NADH to NAD^+, which may be responsible for the cytotoxicity. The reactivity studies showed that conversion to hydroquinone by reaction with NADH or glutathione is irreversible. Complex **1** is not cytotoxic up to 100 μM in normoxia or hypoxia. Complex **1** displays irreversible redox behavior in cyclic voltammetry displaying two overlapping oxidation peaks at 1.00 and 1.57 V w.r.t. NHE, which may be assigned to the conversion of hydroquinone to quinone and Ru^{II} → Ru^{III} respectively.

1. Introduction

Quinones are important redox active compounds in cell signalling processes, mainly in electron transport chain to produce energy in mitochondria.[1] It is known that quinone based ligands have rendered metal complexes with versatile activity in catalysis, [2, 3] molecular magnetism.[4-6] The quinones themselves [7] and their metal complexes have shown broad spectrum of activities and most importantly in therapeutics which includes anti-bacterial, [8, 9] anti-inflammatory, [10, 11] antifungal, [8, 12] and anticancer activities [13-15]. Anthracyclines (viz. doxorubicin, daunorubicin, idarubicin and mitoxantrone) also bear quinone-hydroquinone motifs and have been very successful in clinic for anticancer efficacy.[16] The quinone derivatives (viz. aminonaphthoquinones, [17, 18] sulfonamides, [19, 20] mono oximes [21]) are already known to provide potent anticancer activity. Very importantly, α and β-Lapachones are in clinical trial phase I for the treatment of advanced solid tumours [22, 23] and have shown positive effects in controlling obesity.[24] Quinones have been found to inhibit topoisomerases.[25] Quinones may also follow other pathways of cytotoxicity in a cellular environment. The quinones may get activated by cellular one electron reductases [26, 27] to form semiquinone which reacts with molecular oxygen to generate superoxide while converting itself back to quinone. Thus, ROS generation can happen catalytically. Quinones upon complexation with metal ions show change in redox activity.[28-32] Pt(II) and Ru(II) complexes of 1,2- or 1,4-quinones have been found to exhibit redox potential within the range of ± 0.5 V [28, 33] which should help them to interfere with various physiological processes.[34] The studies show that the metal complexes of quinone based ligands may be reduced to semiquinones which are useful for generation of reactive oxygen species and rendering oxidative damage.[35] The literature show that most metal quinone complexes are rich in redox activity within the physiological range of ± 0.5 V.

Ru(II) has also been found to be an useful alternative to Pt(II) in design of anticancer chemotherapeutic agents.[36-40] Ru(II)-*p*-cymene complexes have provided a large pool of molecules which show diverse mechanism of action. This is achieved by variation in the bidentate coordinating ligand. The redox potential data of the quinone based Ru(II) complexes suggest that complexation may be very useful in generation of hypoxia activable metal complexes. The presence of quinones help in the disruption of cellular redox balance by oxidising cellular NADH to NAD^+ and the metal ion may participate in DNA cross-linking, thereby inducing cytotoxicity through multiple pathways. A quinone may also get

deactivated to hydroquinone through two electron reduction by NAD(P)H: quinoneoxidoreductase 1 (NQO1).[41] However, if the process is reversible then it may also generate ROS while converting back to quinone. Thus, the reduction potential, metal in complexation, stability of the reduced and oxidized species and availability of substrate or the enzyme would dictate the chemistry inside cellular environment.

Hypoxia activation of quinone is an important factor in cancer since tumours become hypoxic due to high rate of proliferation leading to constriction of blood vessels, depriving them of nutrients and oxygen.[42, 43] It is desired that a compound is more active under hypoxia so that it displays more efficient anticancer activity in tumours.[44] The exploration for quinones and their metal complexes are useful for this purpose. Here in, we have synthesized hydroquinone and quinone based compounds, 2,3-bis(3,5-dimethyl-1H-pyrazol-1-yl)benzene-1,4-diol (H_2L1) and 2,3-bis(3,5-dimethyl-1H-pyrazol-1-yl)cyclohexa-2,5-diene-1,4-dione (L2) and a metal complex [Ru(II)(*p*-cym)(H_2L1)Cl](PF_6) (**1**) (Scheme 1). We have studied the compounds and the metal complex for their stability, redox activity and cytotoxicity in normoxia and hypoxia.

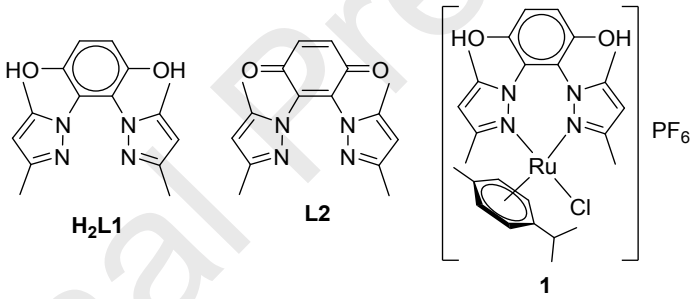

Scheme 1. Chemical structures of Ligands (H_2L1 and L2) complex **1**.

2. Experimental Section

2.1 Materials and Methods: Chemicals and solvents were purchased from various commercial sources (SigmaAldrich, Merck, Spectrochem or SRL). Unless mentioned specifically, the products were used as received. The solvents used for synthetic and analytical purposes were dried or distilled prior to use following standard procedures.[45] Ruthenium trichloride was purchased from Precious Metals Online, Australia and the precursor, $[Ru^{II}_2(\eta^6\text{-}p\text{-cym})_2Cl_4]$ was synthesized as per procedure mentioned in literature.[46] The medium, Dulbecco`s Modified Eagle Media (DMEM) and Dulbecco`s Modified Eagle Media/ Ham's F-12 (DMEM/F12) used for cell culture was purchased from Invitrogen or Sigma Aldrich and Foetal bovine serum (FBS) was obtained from Gibco. UV-

visible spectra were recorded in a Cary300 UV-visible spectrophotometer using spectroscopy grade solvents. FT-IR measurements were done with KBr pellets using a Perkin-Elmer SPECTRUM RX I spectrometer. ^{1}H NMR and ^{13}C NMR were recorded either in JEOL ECS 400 MHz or in Bruker Avance III 500 MHz spectrometer at 25 °C. The chemical shift values are reported in ppm. All the NMR were performed in liquid state after dissolving in deuterated solvents of Cambridge Isotope Laboratories, Inc. The purity of the bulk samples was confirmed after elemental analysis in Perkin-Elmer 2400 series II CHNS/O analyser and through high resolution ESI-MS (Electrospray ionization mass spectra). The HRMS spectra were recorded using a maXis impact (Bruker) mass spectrometer by +ve mode electrospray ionization and plotted using Bruker Daltonics software provided by Bruker. Melting point or decomposition temperature of complex was measured by Secor India melting point apparatus, mean of three independent measurements are reported without any standard deviation. The synthesized compounds were dried under vacuum and stored in desiccator under dark until they were used for experiments.

2.2 Syntheses

2,3-bis(3,5-dimethyl-1H-pyrazol-1-yl)benzene-1,4-diol (H_2L1): Hydroquinone compound H_2L1 was synthesized using previously reported procedure.[2, 47] Yield (25%); ^{1}H NMR (500 MHz, $CDCl_3$, 25 °C): δ 7.25 (s, 2H, OH), 7.04 (s, 2H, ArH), 5.89 (s, 2H, Pyrazole-H), 2.28 (s, 6H, $2CH_3$), 1.67 (s, 6H, $2CH_3$); ^{13}C NMR (125 MHz, $CDCl_3$, 25 °C): δ 151.20, 145.74, 143.76, 120.46, 118.06, 107.02, 13.31, 10.72; ESI-HRMS (Methanol) m/z (calc.): 321.1358 (321.1322) [$C_{16}H_{18}N_4O_2Na^+$]; FT-IR (KBr pellets, cm^{-1}): 3414 ($\nu_{O\text{-}H\ stret.}$), 1501 ($\nu_{arene\ C=C\ stret.}$), 1385 ($\nu_{C\text{-}N\ stret.}$).

2,3-bis(3,5-dimethyl-1H-pyrazol-1-yl)cyclohexa-2,5-diene-1,4-dione **(**L2**):** Ligand L2 was synthesized from hydroquinone compound H_2L1 by 2,3-Dichloro-5,6-dicyano-1,4-benzoquinone (DDQ) oxidation method. 1 mmol DDQ was added to the 15 mL dichloromethane solution of the 1 mmol of hydroquinone ligand (H_2L1) and stirred for 4 h under dark. The completion of the reaction was confirmed by TLC and the product was purified by silica flash column chromatography using ethyl acetate as eluent. Yield: 85 %, ^{1}H NMR (500 MHz, $CDCl_3$, 25 °C): δ 7.00 (s, 2H, Ar-H), 5.87 (s, 2H, Pyrazole-H), 2.13 (s, 6H, CH_3), 2.00 (s, 6H, CH_3) ppm (Fig. S1); ^{13}C NMR: (125 MHz, $CDCl_3$, 25 °C): δ 182.2, 151.6, 143.5, 137.4, 136.0, 107.6, 13.6, 11.4 ppm (Fig. S2); ESI-HRMS (Methanol) m/z (calc.):

319.1202 (319.1165) [$C_{16}H_{16}N_4O_2Na^+$]; FT-IR (KBr pellets, cm^{-1}): 1666 ($\nu_{C=O\ stret.}$), 1563 ($\nu_{arene\ C=C\ stret.}$), 1394 ($\nu_{C-N\ stret.}$).

[Ru(η^6-*p*-cymene)(H_2L1)Cl](PF_6) (**1**): The methanolic solution of ligand L2 (0.3 mmol) was added to the 15 mL of methanolic solution of [$Ru^{II}_2(\eta^6$-*p*-cym)$_2Cl_4$] (0.15 mmol) and refluxed for 3 h in dark, followed by addition of 0.3 mmol of NH_4PF_6 and stirred at room temperature for another 1 h. After evaporation of the reaction solution a deep red coloured mass was obtained. The deep red coloured mass was re-dissolved in dicholoromethane and filtered. The filtrate was evaporated. Finally, the product was purified by washing several times with diethyl ether. Yield: 48 %, Anal. Calc. for $C_{26}H_{30}ClF_6N_4O_2PRu$: C, 43.86; H, 4.25; N, 7.87; Found: C, 43.98; H, 4.24; N, 7.90 %; m.p.: 164 °C (decomp.); ^{1}H NMR (500 MHz, $CDCl_3$, 25°C): δ 7.37 (s, 2H, Ar-H), 6.27 (s, 2H, Pyrazole-H), 5.61 (d, 2H, J = 6.1 Hz, *p*-cym-H), 5.31 (d, 2H, J = 6.1 Hz, *p*-cym-H), 2.64 (m, 1H, *i*Pr-CH), 2.60 (s, 6H, CH_3), 2.20 (s, 6H, CH_3), 1.84 (s, 3H, *p*-cym-CH_3), 1.11 (d, 6H, J = 7.0 Hz, *i*Pr-CH_3) ppm (Fig. S3); ^{13}C NMR: (125 MHz, $CDCl_3$, 25°C): δ 181.0, 161.9, 150.2, 138.2, 137.3, 112.8, 105.4, 103.0, 84.1, 81.8, 31.4, 22.5, 18.7, 18.2, 12.6 ppm (Fig. S4); ESI-HRMS (Methanol) m/z (calc.): 569.1237 (569.1252) [$C_{26}H_{32}ClN_4O_2Ru^+$]; UV-vis: [MeOH, λ_{max}, nm (ε/dm^3 mol^{-1} cm^{-1})]: 313 (7116), 507 (2141); FT-IR (KBr pellets, cm^{-1}): 3141 ($\nu_{C-OH\ stret.}$), 1564 ($\nu_{arene\ C=C\ stret.}$), 1402 ($\nu_{C-N\ stret.}$).

2.3 Stability studies and reactivity of L2 and its Ru Complex

2.3.1 Studying complexation of L2 with [Ru_2(*p*-cym)$_2Cl_4$]: 12 mM CD_3OD solution of L2 was mixed with 0.6 mM CD_3OD solution of [Ru_2(*p*-cym)$_2Cl_4$] at 25 °C. The 20:1 concentration ratio of L2 and Ru-dimer precursor was taken to check whether the transformation is catalytic. First ^{1}H NMR spectrum was recorded within 5 mins of mixing. The NMR tube containing the solution was then incubated at 40°C in dark and spectra were recorded at different time point. After 24h a small portion of the reaction solution was diluted with methanol and the ESI mass spectrum was recorded. The individual ^{1}H NMR spectra of L2, H_2L1 and **1** in CD_3OD were recorded at 25°C for comparison purpose. After 24h, an aliquot of the solution was diluted in methanol and ESI-MS studies were performed.

2.3.2 Stability studies of L2 and 1: The stability study of L2 or **1** in CD_3OD was monitored by ^{1}H NMR. L2 or **1** were dissolved in CD_3OD at 25°C and within 5 min the ^{1}H

NMR spectrum was recorded. The respective NMR tubes containing the solution of L2 and **1** was then incubated at 40°C in dark and spectra were recorded at different time point. After 24h an aliquot of the reaction solutions were respectively diluted with methanol and the ESI mass spectrum recorded within 5 min. The stability of L2 in $CDCl_3$ was also studied by ^1H NMR at 25°C.

2.3.3 Studying complexation of L2 with $[Ru_2(p\text{-cym})_2Cl_4]$ by ESI-MS: The reaction between L2 and $[Ru_2(p\text{-cym})_2Cl_4]$ precursor was also monitored by ESI-MS in methanol at different time point by mixing ca. 1:0.5 molar equivalent of L2 and $[Ru_2(p\text{-cym})_2Cl_4]$at 25°C. The ESI mass spectra were recorded immediately after addition and monitored over time.

2.3.4 Complexation of L2 with $[Ru_2(p\text{-cym})_2Cl_4]$ in $CDCl_3$: The complexation of L2 with $[Ru_2(p\text{-cym})_2Cl_4]$ was also monitored in $CDCl_3$ to check the importance of methanol. In this case, 12 mM $CDCl_3$ solution of L2 was mixed with 3 mM $CDCl_3$ solution of $[Ru_2(p\text{-cym})_2Cl_4]$ at 25°C. After immediate mixing, the ^1H NMR spectrum was recorded. The mixture was incubated at 25°C in dark and ^1H NMR spectra were recorded at different time point. After 24h of reaction ESI mass spectrum was taken by dilution with acetonitrile to avoid any methanol involvement. The individual ^1H NMR spectra of L2 and **1** in $CDCl_3$ were recorded at 25 °C for comparison purpose.

2.3.5 Investigation of oxidation of methanol by L2: The reduction of L2 by methanol in CD_3OD demanded investigation of formaldehyde formation. A solution of L2 was made in CH_3OH-CD_3OD (5:1 *v/v*) and incubated for 15 min at 40 °C. The ^1H NMR was recorded for formation of formaldehyde.

2.4 X-ray Crystallography

The single crystals of ligand L2 was obtained from dichloromethane solution at 4 °C. Complex **1** gave crystals from dichloromethane solution layered with hexane and kept at 4 °C. A block shaped single crystal of dimension 8.57 × 13.35 × 13.00 (L2) or 11.71 × 13.29 × 18.57 (**1**) was mounted on a loop using fomblin oil on a SuperNova, Dual, Cu at zero, Eos diffractometer. The data was collected either at 100 K (L2) or at 293 K (**1**) using Mo X-ray source of wavelength 0.71073 Å. The diffraction data was integrated in CrysAlisPro 171.37.33c and solved with ShelXS using direct methods.[48] Whereas the structure was refined with ShelXL using least squares minimisation.[48] Data was processed using Olex2 software package.[49] Non-hydrogen atoms were refined anisotropically using full matrix

least-squares on F^2. The ORTEP diagram of the ligand and complex are represented with 50 % probability thermal ellipsoids. Some important crystallographic parameters are listed in Table S1. The CCDC numbers of ligand (L2) and Complex **1** are 1943935 and 1943936 respectively.

2.5 Cyclic voltammetry

Cyclic voltammetry studies were performed for L2 using CHI604D electrochemical work station. Glassy carbon was used as working, platinum wire as counter and a non-aqueous Ag/Ag^+ as reference electrode. 0.1 M TBAP was the supporting electrolyte and acetonitrile was used as solvent. A scan rate of 50 mV s^{-1} was used to collect data for intact complex and ligand. The cyclic voltammetry for the reaction of L2 with 1 equivalent of NADH was studied in 1:1 (*v/v*) MeCN : 20 mM Phosphate buffer (pH 7.4) solution at a scan rate of 100 mV s^{-1}. The potential of Ag/Ag^+ reference electrode is calculated to be 0.540 V with respect to NHE based on the $E_{1/2}$ obtained for Fe^{III}/Fe^{II} couple of ferrocene. All potential values reported are with respect to NHE.

2.6 NMR studies

2.6.1 Hydrolysis: The aqueous stability was studied for complex **1** using 9 : 1 (*v/v*) 10 mM phosphate - 4 mM saline buffer (pD = 7.4) and CD_3OD mixture at 25 °C. The stability was monitored by ^1H NMR at different interval of time for a period of 24 h.

2.6.2 Reduction with NADH: The reduction of quinone ligand (L2) by NADH was monitored by ^1H NMR. The study was performed in 10% CD_3OD in 10 mM phosphate buffer (pD 7.4) having 4 mM NaCl. L2 were allowed to react separately with 2 equivalents of NADH.

2.6.3 L-Glutathione (GSH) and Cysteine binding: The binding was monitored by ^1H NMR. The quinone ligand (L2) was allowed to react with 1 equivalent of thiol (GSH or cysteine) in a mixture of 10% MeOD - 10 mM phosphate buffer of pD 7.4 having 4 mM NaCl. The studies were performed at 25 °C.

2.7 Cell lines and cell culture

Cancer cell lines were obtained from National Centre for Cell Science (NCCS), Pune, India. Human metastatic breast adenocarcinoma (MDA-MB-231), Human pancreatic carcinoma (MIA PaCa-2) cells were maintained in DMEM/F12 and DMEM medium

containing 10 % FBS and 1 % antibiotic-antimitotic solution respectively. The hypoxic condition was achieved by maintaining 5% carbon dioxide and 1.5% oxygen level. 5% carbon dioxide and 17 % oxygen level were used for normoxia at 37 °C.

2.8 Cell viability assay

The toxicity of the complexes was determined by MTT assay. Briefly, 6×10^3 cells were seeded in each well of 96 well plate and incubated for 48 h at 37 °C (5% CO_2 atmosphere). After 48 h the media was replenished, and complex solution was added. Complex solution was prepared in DMSO and diluted with the culture medium so that the DMSO concentration is each well less than 0.2 %. After 48 h of incubation with complex, media was removed. Fresh medium containing 0.02 mg MTT was added to each well and incubated for further 3 h. The media was then removed and 200 µL DMSO was added in each well. The cells lysed and the formazan crystals dissolved in DMSO. The absorbance was taken at 515 nm in SpectraMax M2e Microplate reader. The IC_{50} values were obtained by 4 parameters fitting. The graphs are plotted as % cell viability vs. logarithmic concentration of complex using GraphPad Prism 5. The IC_{50} value of L2 and **1** against MiaPaCa-2 and MDA-MB-231, under normoxic condition, was also determined by making stock solutions of the compounds in ethanol and diluting it with cell culture medium using the same procedure mentioned above.

2.9 ROS generation

5×10^4 MDA-MB-231 cells were seeded in each well of a 6 well plate and incubated at 37 °C in DMEM/F12 medium. After 48 h media was replenished and cells were incubated with IC_{50} and IC_{25} concentrations of ligand (L2) for 6 h at 37 °C in DMEM/F12 medium. Cells were harvested and washed twice with 1X PBS. The resultant cell pellet was re-suspended in 1X PBS (pH 7.4) containing 10 µM DCFH-DA and incubated for 30 minutes under dark at 37 °C. The intracellular ROS generation was measured by BD Biosciences FACS Calibur flow cytometer.

The change in ROS accumulation was investigated in various ways: (1) by use of the antioxidant and cellular GSH inducer, N-acetylcysteine (NAC).[50, 51] Cells were pre-incubated with 500 µM of NAC for 12 h and then treated with L2 (IC_{50} dose), (2) In another experiment, cells were co-incubated with 500 µM of GSH and IC_{50} conc. of L2 for 6 h at 37

°C, (3) Lastly, cells were also independently co-incubated with 100 µM of NADH and IC_{50} dose of L2 for 6 h at 37 °C.

The resultant cells were harvested and washed twice with 1X PBS and the cell pellet re-suspended in 1X PBS (pH 7.4) containing 10 µM DCFH-DA and incubated for 30 minutes under dark at 37 °C. The intracellular ROS generation was measured by BD Biosciences FACS Calibur flow cytometer.

3. Results and discussion

3.1 Synthesis and characterisation

The synthesis of complex **1** was initiated with L2. However, during synthesis, L2 reduced to H_2L1 and gave complex **1**, $[Ru^{II}(H_2L1)(\eta^6\text{-}p\text{-cym})Cl](PF_6)$ (Scheme 2). Since the oxidation state of Ru^{II} did not change so we performed the necessary NMR and ESI-MS based experimentation (discussed later in this section), which shows the involvement of methanol in the reduction process and formation of formaldehyde due to oxidation of methanol. The ligands and the Ru(II) complex were characterized by ^1H and ^{13}C NMR, (Fig. S1 to S4), HRMS, FT-IR, elemental analysis, UV-vis and single crystal x-ray diffraction. The HRMS data obtained from the methanolic solution of **1** corresponded with m/z, 569.1237 (calc. 569.1252) of formulae $[Ru^{II}(H_2L1)(\eta^6\text{-}p\text{-cym})Cl]^+$. The UV-vis spectra showed a weak metal to ligand charge transfer band at 507 nm and a $\pi \rightarrow \pi^*$ transition at 313 nm. The IR spectra of **1** displayed a band at 3141 cm^{-1} corresponding to the $\nu_{O\text{-}H}$ stretching, similar to H_2L1 which was substituted by a $\nu_{C=O}$ at 1666 cm^{-1} in L2. The $\nu_{C=O}$ stretching was not found in **1** which supported the reduction of the quinone to hydroquinone during synthesis.

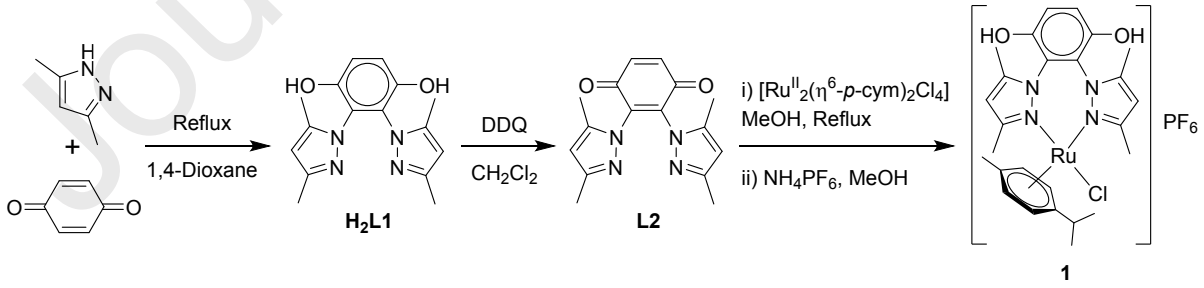

Scheme 2. A representation of the synthesis of complex **1**.

Complex **1** showed stability in methanolic solution (Fig. S5). NMR studies were performed to confirm the reduction of quinone moiety of L2 to hydroquinone H_2L1 in

methanol in the presence of $[Ru_2(p\text{-cym})_2Cl_4]$, either by catalytic transformation or by stoichiometric transformation. To check this, we mixed L2 and $[Ru_2(p\text{-cym})_2Cl_4]$ in CD_3OD at 25 °C in 20:1 molar ratio respectively and immediately recorded ^1H NMR to find the formation of $[Ru(p\text{-cym})(L2)Cl]^+$ (Fig. 1). Then the same solution was incubated at 40 °C (temperature used during synthesis) and the ^1H NMR spectra started to exhibit formation of the hydroquinone complex $[Ru(p\text{-cym})(H_2L1)Cl]^+$ (Fig. 1) with time and oxidised the solvent CD_3OD to $D_2C{=}O$ (confirmation through a separate experiment using CH_3OH which is described later in this section). The same solution was injected in ESI-MS after 24 h upon dilution with methanol and a m/z of 330.1705 (calc. 330.1671) corresponding to the formulation $[H_2DL1\text{-}OMe]^+$ apart from the $[Ru(p\text{-cym})(H_2L1)Cl]^+$, m/z of 569.138 (calc. 569.126) was observed. Apart from the above the presence of free quinone (L2) and hydroquinone (H_2L1) ligand was also detected.

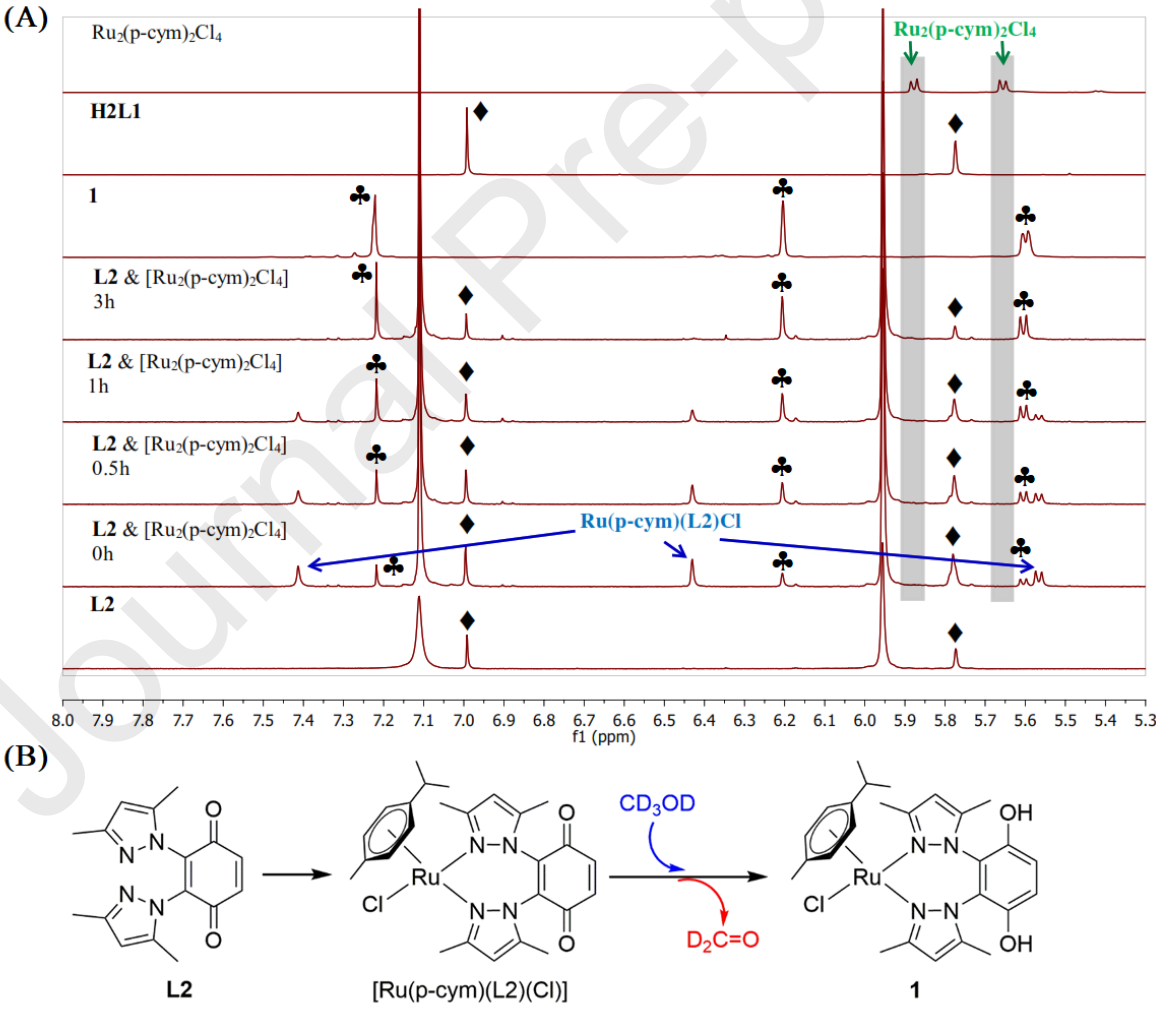

Fig. 1. Complexation of L2 with $[Ru_2(p\text{-cym})_2Cl_4]$ in CD_3OD monitored by ^1H NMR. (A) '♦' indicates formation of H_2L1, '♣' indicates the formation of complex **1** (B) A schematic representation of the reduction reaction.

In the NMR tube no further conversion of L2 to free H_2L1 occurred after complete consumption of the $[Ru_2(p\text{-cym})_2Cl_4]$ (Fig. 1) within 3h. It seemed as if the Ru-dimer precursor is involved in the quinone reduction process. In order to understand the fate of the free ligand in absence of the $[Ru_2(p\text{-cym})_2Cl_4]$, we have performed the stability study of L2 in CD_3OD monitored by ^1H NMR (Fig. 2). Slow transformation of L2 to H_2L1 was observed even at 25 °C. After 6h, almost full conversion and a deuterated methoxy adduct was detected (Fig. 2). One of the ortho position to the 1,4-quinone in L2 reacted with the CD_3OD, evident from the absence of the corresponding hydrogen, clearly visible in the ^1H NMR (Fig 2C). The absence of proton signals of methoxy methyl in the ^1H NMR, indirectly suggests the presence of the deuterated methoxy adduct. The same adduct of formulation $[H_3L1\text{-}OCD_3]^+$ corresponding to m/z of 332.1797 (calc. 332.1796) was also confirmed by ESI-MS (Fig. S9 and S10). Hence, the solvent methanol is readily assisting the reduction of the quinone ligand to hydroquinone which was inhibited in presence of the $[Ru(p\text{-cym})(L2)Cl]^+$ and $[Ru(p\text{-cym})(H_2L1)Cl]^+$. Thus, the Ru-quinone and hydroquinone complexes behave as catalytic poisons.

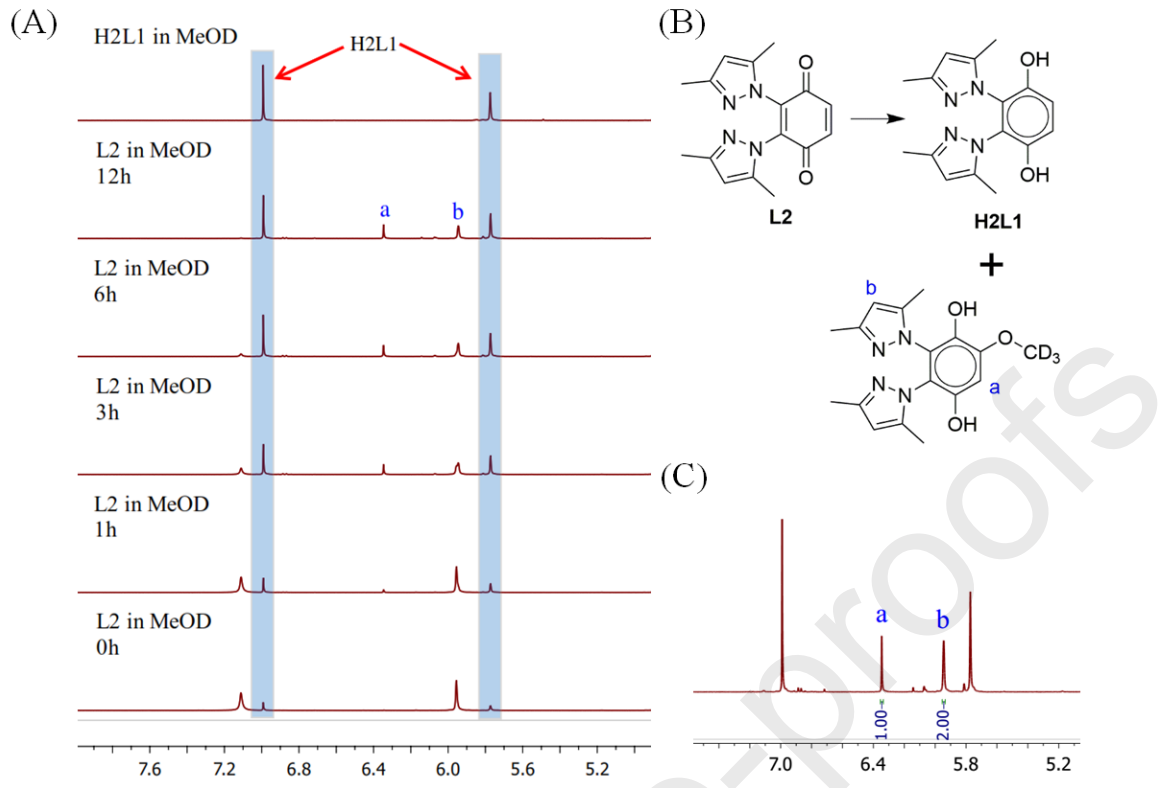

Fig. 2. Stability study of L2 in CD_3OD measured by ^1H NMR. (A) time dependent plot of the reaction showing reduction to H_2L1 as depicted by the highlighting band (B) A scheme of the monitored reduction reaction (C) A zoomed view of the integration of the two important protons for comparison

The involvement of methanol for this quinone-hydroquinone transformation process was further confirmed by the stability study and reaction kinetics between L2 and Ru-dimer precursor in the non-methanolic solvent, $CDCl_3$. The ligand L2 in $CDCl_3$ showed stability over 24h (Fig. S11). The complexation between L2 and Ru-dimer precursor in $CDCl_3$ led to the slow formation of $[Ru(p\text{-cym})(L2)Cl]^+$ (Fig. S12). Interestingly, no further reduction of $[Ru(p\text{-cym})(L2)Cl]^+$ to $[Ru(p\text{-cym})(H_2L1)Cl]^+$ was detected (Fig. S12) which is attributed to the absence of methanol. The ESI-MS study of the same solution (diluted in acetonitrile) indicate the formation of $[Ru(p\text{-cym})(H_2L1)Cl]^+$ instead of $[Ru(p\text{-cym})(L2)Cl]^+$ (Fig. S13 to S15), although no such peaks corresponding to complex **1** were detected in ^1H NMR (Fig. S12). This indicates the reduction of quinone species can also occur under ESI-MS conditions.

The formation of the Ru-quinone complex and its conversion were monitored under ESI-MS conditions in methanol. The freshly prepared precursor solution of $[Ru_2(p\text{-cym})_2Cl_4]$ in methanol and freshly prepared methanolic solution of L2 with ca. 0.5:1 molar ratio were

mixed and immediately ESI mass spectrum was recorded (Fig. S8). The ESI mass spectra of the mixture were recorded at different time points. The first spectrum was evident for the initial formation of Ru-quinone complex $[Ru(p\text{-cym})(L2)Cl]^+$ (m/z 567.1181) (Fig. S8 indicated by red arrow). Then the peaks corresponding to $[Ru(p\text{-cym})(H_2L1)Cl]^+$ (m/z 569.1204) started to appear (Fig. S8 indicated by green arrow) suggesting that either the ligand was reduced and then complexed with the Ru(II) or the $[Ru(p\text{-cym})(L2)Cl]^+$ was reduced to $[Ru(p\text{-cym})(H_2L1)Cl]^+$ similar to what was observed in ^{1}H NMR (Fig S8).

The formation of formaldehyde from methanol, during reduction of quinone (L2) to hydroquinone (H_2L1) was also confirmed by ^{1}H NMR (Fig. S16) by dissolving L2 in a 5:1 *v/v* CH_3OH:CD_3OD mixture and incubation for 15 min at 40 °C. A new peak appeared at 9.16 ppm corresponding to formaldehyde. This peak was absent both in free hydroquinone ligand (H_2L1) and L2 in CD_3OD (Fig. S16). Hence, the peak is corresponding to formaldehyde and not for the –OH of hydroquinone. Literature data also shows that the ^{1}H NMR peak for formaldehyde appears in the same region.[52, 53] Importantly, the integration of the peak for the two protons of formaldehyde is 1.67 whereas for the two aromatic hydrogens it is 2, which is due to use of 17% CD_3OD.

3.2 X-ray Crystallography

The quinone-bis(pyrazole) ligand L2 crystallized in monoclinic system with space group *I*2/a (Table S1) where the sp^2 hybrized N-donors of pyrazole are present in an orientation not suitable for metal binding. Each unit cell of L2 contains 4 molecules. Each oxygen of quinone simultaneously forms two intermolecular H-bonding with pyrazole ring-H and one CH_3 of pyrazole with average distances ca. 3.38 Å (Fig. S17). During complexation, sp^2 hybrized N-donors re-orient themselves to form the N,N chelated complex **1**, which crystallizes in a monoclinic system with space group $P2_1/c$ (Table S1). The crystals of **1** were obtained by layering a dichloromethane solution with hexane. The structure of **1** shows a distorted tetrahedral geometry around the metal centre (Fig. 3) and a PF_6^- anion in the lattice. Each unit cell contained four molecules of **1**. In complex **1,** interaction of an oxygen of the hydroquinone with -CH_3 of *p*-cymene (distance 3.183 Å) is observed (Fig. S18).

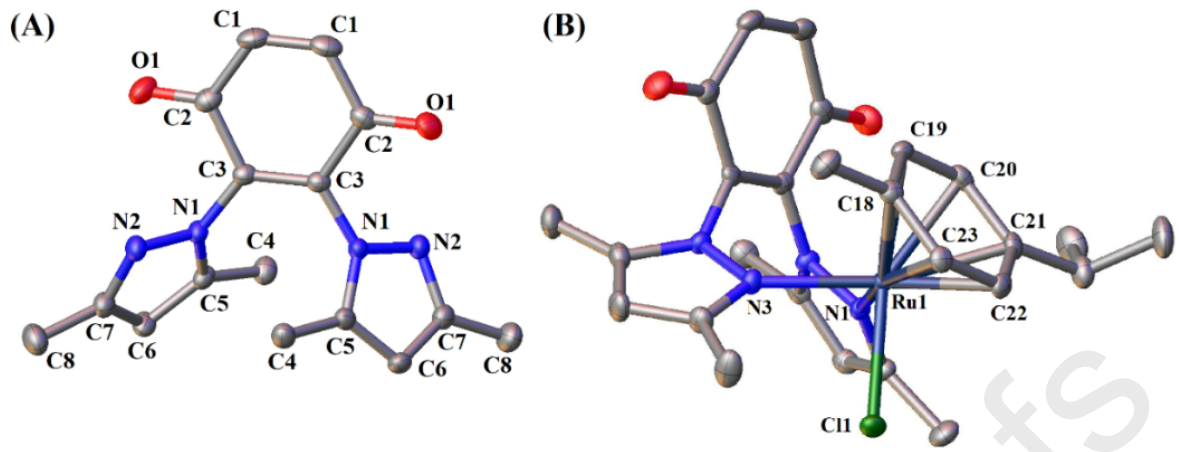

Fig. 3. Molecular structure of (A) ligand (L2) and (B) complex **1** with 50% probability level thermal ellipsoids**.** All hydrogen atoms and counter anion are omitted for clarity.

Table 1

Selected bond lengths (Å) of ligand L2 and complex **1**.

L2		**1**	
O1 C2	1.222(2)	O2 C8	1.223(4)
N1 N2	1.3786(19)	Ru1 N1	2.158(3)
N1 C3	1.4035(19)	Ru1 N3	2.156(3)
N1 C5	1.372(2)	Ru1 Cl1	2.3919(8)
C3 C2	1.498(2)	Ru1 C18	2.217(3)
C1 C2	1.457(2)	Ru1 C19	2.207(3)
C6 C7	1.407(2)	Ru1 C20	2.199(3)
C6-C5	1.361(2)	Ru1 C21	2.230(3)
C7 C8	1.493(2)	Ru1 C22	2.184(3)
C5 C4	1.490(2)	Ru1 C23	2.185(3)

Table 2

Selected bond angles (°) of ligand L2 and complex **1**.

L2		**1**	
N2 N1 C3	117.35(12)	N3 Ru1 N1	86.22(10)
C5 N1 N2	112.41(13)	N1 Ru1 Cl1	86.60(7)
C5 N1 C3	130.23(14)	N3 Ru1 Cl1	85.19(7)

C7 N2 N1	104.03(13)	N1 Ru1 C18	149.70(11)
N1 C3 C2	115.75(13)	N1 Ru1 C19	113.47(11)
O1 C2 C3	120.67(15)	N1 Ru1 C20	91.74(11)
O1 C2 C1	120.95(15)	N1 Ru1 C21	96.72(11)
C1 C2 C3	118.29(15)	N1 Ru1 C22	125.85(12)
C5 C6 C7	106.82(15)	N1 Ru1 C23	163.83(12)
N2 C7 C6	111.43(15)	N3 Ru1 C18	89.04(12)
N2 C7 C8	119.73(16)	N3 Ru1 C19	97.25(12)
C6 C7 C8	128.84(16)	N3 Ru1 C20	127.46(12)
N1 C5 C4	123.18(14)	N3 Ru1 C21	164.61(12)
C6 C5 N1	105.31(15)	N3 Ru1 C22	146.66(11)
C6 C5 C4	131.49(15)	N3 Ru1 C23	109.88(12)

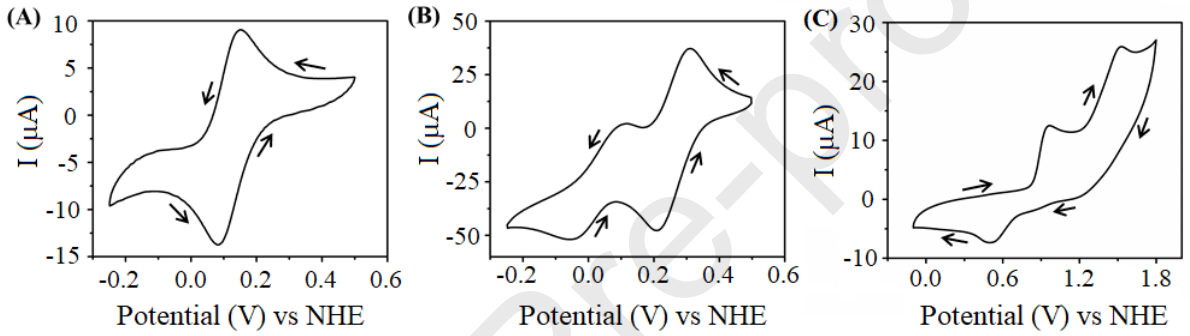

Fig. 4. Cyclic voltammogram of (A) L2 in acetonitrile, (B) L2 and 1 equiv. NADH in 1:1 (*v/v*) MeCN : 20mM Phosphate buffer pH 7.4 and (C) complex **1** in acetonitrile. Reference electrode used was Ag/Ag^{+} whose potential was 0.54 V w.r.t. NHE.

3.3 Electrochemistry

Cyclic voltammograms of a 1 mM acetonitrile solution of L2 showed $E_{1/2}$ 0.12 V and the process was quasi-reversible with ΔEp = 67 mV (Fig. 4). We investigated the influence of NADH on the reduction process and found that in presence of 1 equivalent of NADH the redox process became irreversible in nature ($E_{1/2}$ = 0.03 V). The ΔEp increased from 67 mV to 158 mV. NADH oxidized itself in presence of L2 and reduced it irreversibly to the corresponding hydroquinone (H_2L1). Complex **1** showed two overlapping oxidation process with peaks at 1.00 and 1.57 V, which may be assigned to the conversion of the hydroquinone to quinone and Ru^{II} → Ru^{III} respectively. Along with that, two less prominent reduction peaks at 1.25 and 0.54 V was observed. The higher ΔEp of the redox process and a large variation

in the peak currents, i_{pa} and i_{pc}, suggested that the electrochemical redox process may be coupled with chemical events and irreversible.

3.4 Stability studies

The solution stability of complex **1** in aqueous medium was investigated using CD_3OD : 10 mM phosphate, 4 mM saline buffer at pD 7.4 (1:9 *v/v*). The ^1H NMR data showed that more than 97% of complex **1** is stable in its native form upto 24 h (Fig. 5). There may be only ca. 3% of hydrolysis in the 24 h period. The reduction potential of L2 ($E_{1/2}$ = 120 mV vs NHE) made it necessary to investigate its reduction in presence of NADH using ^1H NMR. 2 equivalents of NADH was added to the methanolic solution of L2. The solution almost instantaneously changed colour from red to colourless with a white precipitate (some of the hydroquinone precipitated due to lower solubility) (Fig. S20) and peaks corresponding to the

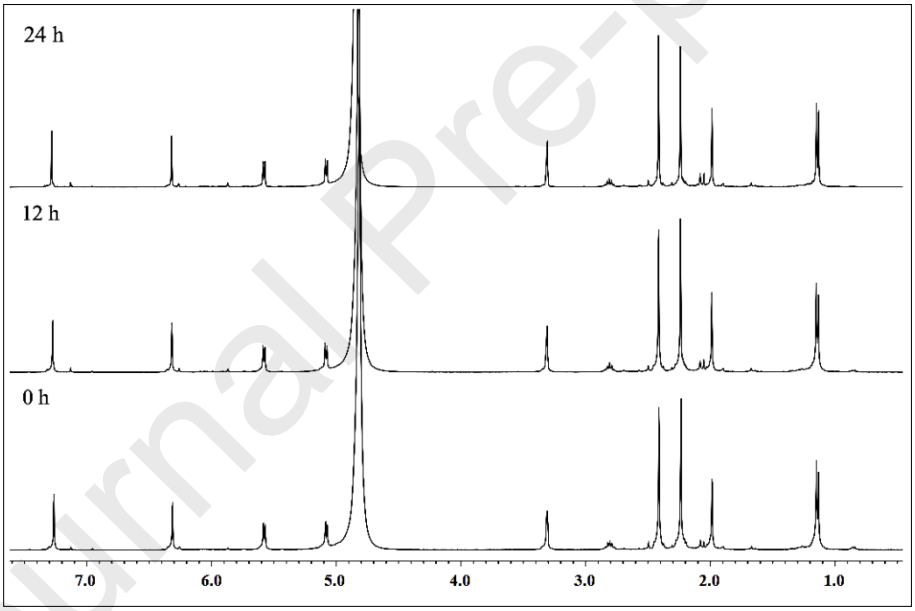

Fig. 5. ^1H NMR spectrum of **1** in CD_3OD : 10 mM phosphate, 4 mM saline buffer at pD 7.4 (1:9 *v/v*) showing complex is stable and stays mostly intact as $[Ru^{II}(H_2L1)(p\text{-cym})Cl]^+$.

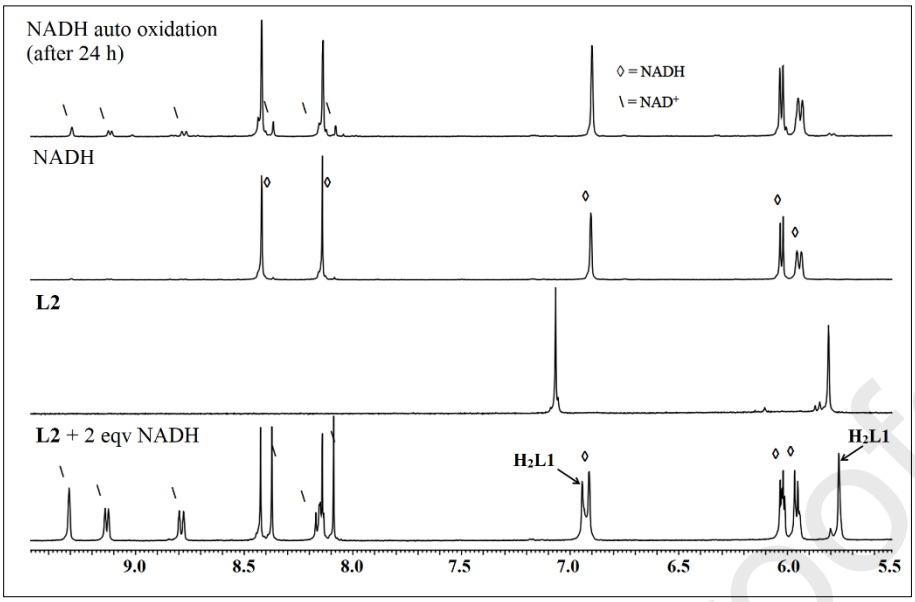

Fig. 6. Stack plot of ^{1}H NMR for reaction of ligand L2 with 2 equivalents of NADH in 10 % CD_3OD in 10 mM phosphate, 4 mM saline buffer (pD 7.4).

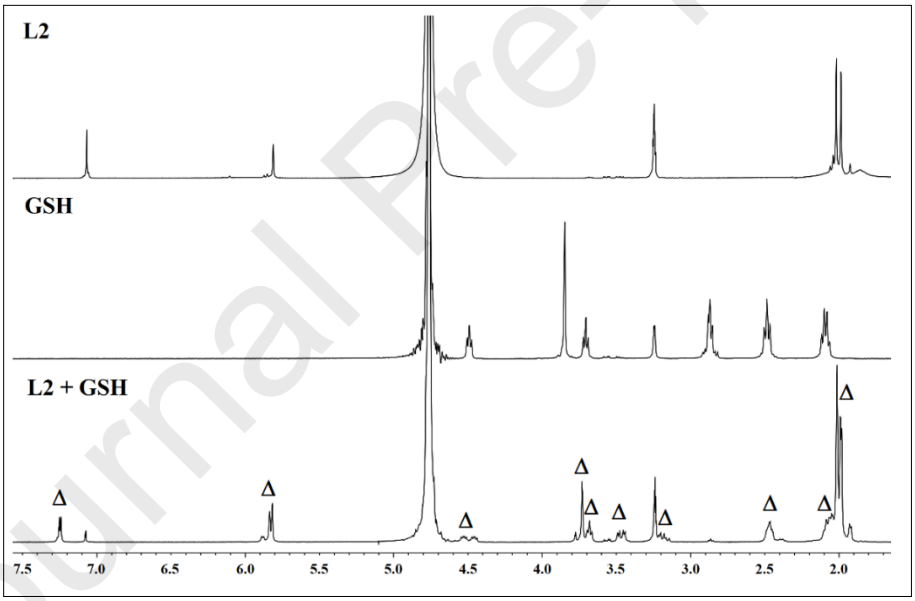

Fig. 7. GSH binding study of L2 with GSH in 10 % MeOD in 10 mM phosphate, 4 mM NaCl buffer (pD 7.4). Where Δ indicate GSH bound species.

hydroquinone H_2L1 appeared in the NMR spectra. Thus, the ability of the quinone ligand (L2) to oxidize NADH to NAD^+ was confirmed by NMR (Fig. 6 and Scheme 4). The ^{1}H peaks corresponding to the remaining hydroquinone in solution was visible in the NMR spectrum (Fig. 6). The quinones are also reactive to thiols [54, 55] and we found L2 to be reactive to the thiols when 1 equivalent of GSH (Fig. 7) or 1 equivalent cysteine (Fig. S19)

was added to an aqueous solution (CD_3OD : 10 mM phosphate, 4 mM saline buffer at pD 7.4) of L2 separately. The resultant thiol adduct was quite soluble in the aqueous phase and hence gave a clear solution (Fig. S20). The thiol binding and ring aromatisation of L2 took place by replacing a hydrogen ortho to the quinone motifs, as revealed through ^{1}H NMR (Scheme 3). Although the thiol reactivity of L2 is observed for the first time but similar reactivities have been earlier reported with other quinone ligands in literature.[55, 56] Complex **1** is also not stable in presence of sulfur based nucleophiles (viz. DMSO, GSH) and degrades quickly.

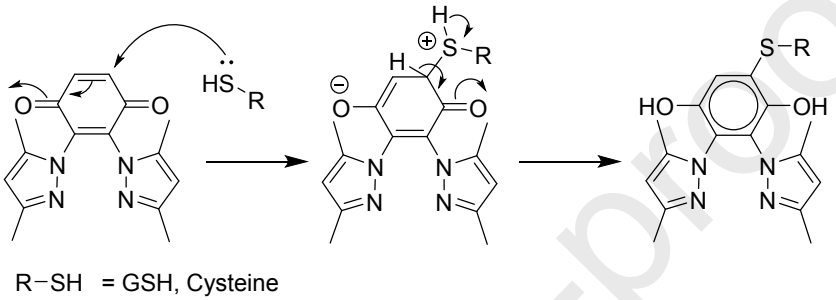

Scheme 3. A scheme depicting the possible mode of reaction of thiols with L2 to form adducts.

Table 3

Cytotoxicity of ligands and complex **1**.

Complex	IC_{50} ± S.D.[a] (μM)			
	Normoxia[b]		Hypoxia[c]	
	MIA PaCa-2	MDA-MB-231	MIA PaCa-2	MIA PaCa-2 + NAC[d]
1	>100	>100	>100	>100
H_2L1	>200	>200	>200	N.D.[e]
L2	155.2 ± 3.2	122.9 ± 1.8	58.5 ± 5.1	104.2 ± 0.7
CDDP	31.8 ± 5.0	37.2 ± 2.5	18.1 ± 2.9	29.7±4.1[f]

[a]S.D. means standard deviation, [b]IC_{50} was determined under normoxic conditions. [c]IC_{50} was determined under hypoxic conditions (1.5 % O_2), [d]cells were pre-incubated with 500 μM N-acetyl cysteine. [e]N.D. means not determined. [f]cisplatin was co incubated with 20 molar equivalents of GSH. Representative plots are provided in Fig. S21.

3.5 Cell viability assay

The ligands H_2L1, L2 and complex **1** were studied for their cytotoxicity against the triple negative breast carcinoma (MDA-MB-231) and the pancreatic carcinoma (MIA

PaCa-2). L2 showed IC_{50} in the range of 123-155 μM. However, when L2 was investigated under hypoxia in MIA PaCa-2 cell line then there was ca. 2.7-fold increase in toxicity (IC_{50} ca. 59 μM) under hypoxic condition (Table 3). In hypoxic condition oxygen percentage is very limited restricting the amount of superoxide formation. In hypoxia, the conversion of quinone to semiquinone may help enhance the ROS population thus increasing toxicity.[57-60] L2 also readily reacted with NADH to form the corresponding hydroquinone while oxidizing the NADH to NAD^+ which would affect both ATP production and cellular redox balance. This may be the reason of the toxicity of L2. The toxicity of L2 and **1** has been also evaluated after dissolving the respective compounds in ethanol (instead of DMSO) against MDA-MB-231 and MIA PaCa-2, under normoxic conditions due to poor stability of **1** in DMSO. The results showed that the IC_{50} (in μM) of **1**, IC_{50} >100 μM and for L2 is same (155 ± 3 in MIA PaCa-2 and 121 ± 4 in MDA-MB-231) (Fig. S22 and S23). We could not investigate **1** beyond 100 μM since it was precipitating out of solution. However, ca. 10-20% cell death was observed at 100 μM suggesting poor toxicity of **1** compared to L2 where at least ca. 25-30 % cell death was observed in MDA-MB-231 or MIA PaCa-2 at 100 μM.

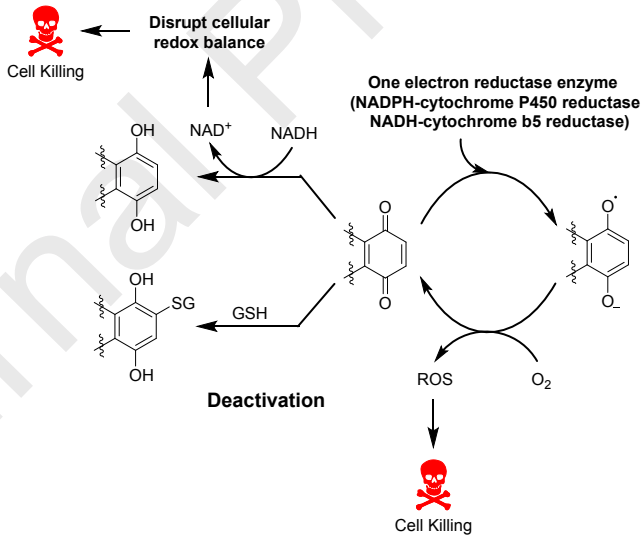

Scheme 4. Activation and deactivation mechanism of quinone systems inside cell.[61, 62]

The DCFH-DA assay to study increase in ROS population showed enhancement of ROS is presence of L2. Hence, ROS is one of the underlying mechanisms of cell killing (Scheme 4 and Fig. 8). The ROS enhancement was investigated in MDA-MB-231 by flow cytometry after 6 h incubation with L2. The green fluorescence increased due to reaction of DCFHDA with ROS suggesting L2 is able to enhance ROS population in cells (Fig. 8A). The quenching

of ROS production was observed when L2 was co-incubated with NADH (Fig. 8B). Similar result was observed in presence of GSH as well as in GSH induced cells for ligand L2 (Fig. 8C). These indicate the reason of deactivation in presence of cellular thiols. Complex **1** in spite of excellent stability in physiological buffer, did not exhibit any cytotoxicity. The probable reasons are its poor redox behaviour and degradation in presence of sulfur based nucelophiles. The results suggest that the complexation with Ru^{II} hampered the redox activity of L2, which is responsible for its poor reactivity and cytotoxicity.

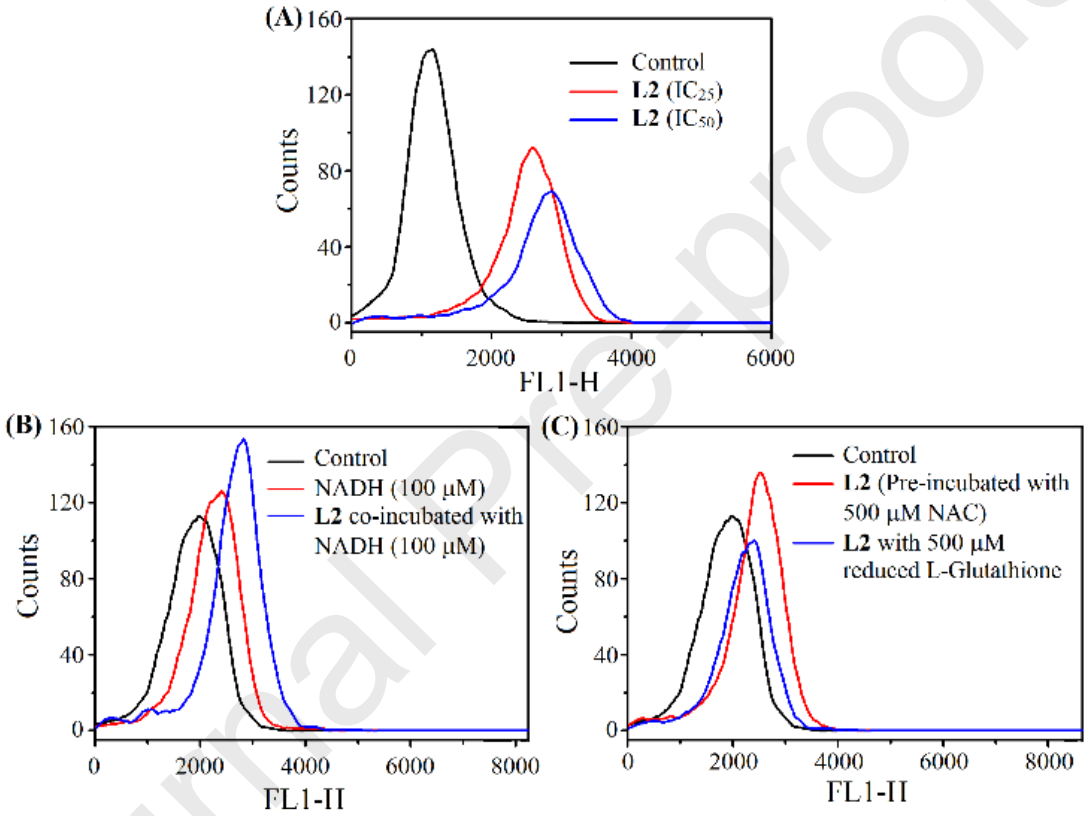

Fig. 8. ROS detection for (A) compound L2. (B) ROS quenching in presence of 100 µM NADH and L2 (IC_{50} dose) in comparison to NADH treated cells and untreated control. (C) ROS quenching by co-incubation of L2 (IC_{50} dose) with 500 µM GSH and cells are pre-incubated with 500 µM NAC.

4. Conclusions

In summary, the quinone L2 reduced to form hydroquinone H_2L1 in methanolic solution and oxidised methanol to formaldehyde. The results obtained from the stability and cytotoxicity profiles suggest that the complexation of the bis(pyrazole) based 1,4-quinone (L2) with Ru^{II} is not suitable for enhancing its anticancer therapeutic efficacy. L2 is redox active and

displays quasi-reversible redox behaviour in cyclic voltammetry with $E_{1/2}$ at 0.12 V, which is within the physiological range. L2 converts NADH to NAD^+ and induces oxidative stress through ROS accumulation which is responsible for its cytotoxicity. The metal complex **1** showed stability at pH 7.4 but is not cytotoxic to cancer cells either in normoxia or hypoxia, whereas L2 is activated in hypoxia by ca. 3 times as per the results obtained in pancreatic carcinoma (MIA PaCa-2). Our studies show that complexation with Ru(II) has diminished activity but there is a scope of improvement in activity by change of metal and tuning the redox potential. In addition, the reactivity with methanol suggests that we may be able to modify the ligand by exploiting the reactivity with alcohols and design a superior ligand that would be less reactive to thiols. We understand that the irreversible reduction of the quinone to hydroquinone by cellular NADH, is a limiting factor in the cytotoxicity profile.

Acknowledgements

We are sincerely acknowledged DST for financial support vide project no. EMR/2017/002324, IISER Kolkata for infrastructure and financial support including the central instrumentation facilities. K.P. thanks UGC and IISER Kolkata, for providing research fellowship.

Appendix A. Supplementary data

CCDC: 1943935 and 1943936 contain the supplementary crystallographic data.

Supplementary data to this article can be found online.

References:

[1] G. Powis, Free Radical Biol. Med., 6 (1989) 63-101.
[2] A. Kumar, K. Purkait, S.K. Dey, A. Sarkar, A. Mukherjee, RSC Adv., 4 (2014) 35233-35237.
[3] A.E. Wendlandt, S.S. Stahl, J. Am. Chem. Soc., 136 (2014) 506-512.
[4] I. Minkin Vladimir, G. Starikov Andrey, A. Starikova Alyona, M. Minyaev Ruslan, I. Boldyrev Alexander, Dalton Trans., 47 (2018) 15948-15956.
[5] U. Albold, C. Hoyer, I. Neuman Nicolas, S. Sobottka, B. Sarkar, I. Neuman Nicolas, S. Hazari Arijit, K. Lahiri Goutam, Inorg. chem., 58 (2019) 3754-3763.
[6] P. Bubnov Michael, K. Cherkasov Vladimir, A. Teplova Irina, O. Druzhkov Nickolay, V. Baranov Evgenii, A. Abakumov Gleb, D. Grishin Ivan, S. Bogomyakov Artem, Dalton Trans., 48 (2019) 10516-10525.
[7] E.A. Hillard, F.C. de Abreu, D.C.M. Ferreira, G. Jaouen, M.O.F. Goulart, C. Amatore, Chem. Commun., (2008) 2612-2628.
[8] J.J. Inbaraj, C.F. Chignell, Chem. Res. Toxicol., 17 (2004) 55-62.

[9] S.-T. Huang, H.-S. Kuo, C.-L. Hsiao, Y.-L. Lin, Bioorg. Med. Chem., 10 (2002) 1947-1952.
[10] V.K. Tandon, R.B. Chhor, R.V. Singh, S. Rai, D.B. Yadav, Bioorg. Med. Chem. Lett., 14 (2004) 1079-1083.
[11] L.-J. Huang, F.-C. Chang, K.-H. Lee, J.-P. Wang, C.-M. Teng, S.-C. Kuo, Bioorg. Med. Chem., 6 (1998) 2261-2269.
[12] K. Sasaki, H. Abe, F. Yoshizaki, Biol. Pharm. Bull., 25 (2002) 669-670.
[13] J.S. Driscoll, Cancer chemotherapy reports. Part 2, 4 (1974) 3-4.
[14] X. Mou, S. Kesari, P.Y. Wen, X. Huang, Int. J. Clin. Exp. Med., 4 (2011) 17-25.
[15] D.S. Shewach, R.D. Kuchta, Chem. Rev., 109 (2009) 2859-2861.
[16] J. Nadas, D. Sun, Expert Opin. Drug Discovery, 1 (2006) 549-568.
[17] D. Bhasin, S.N. Chettiar, J.P. Etter, M. Mok, P.-K. Li, Bioorg. Med. Chem., 21 (2013) 4662-4669.
[18] J. Benites, J.A. Valderrama, K. Bettega, R.C. Pedrosa, P.B. Calderon, J. Verrax, Eur. J. Med. Chem., 45 (2010) 6052-6057.
[19] H.R. Lawrence, A. Kazi, Y. Luo, R. Kendig, Y. Ge, S. Jain, K. Daniel, D. Santiago, W.C. Guida, S.M. Sebti, Bioorg. Med. Chem., 18 (2010) 5576-5592.
[20] K. Xu, Z. Xiao, Y.B. Tang, L. Huang, C.-H. Chen, E. Ohkoshi, K.-H. Lee, Bioorg. Med. Chem. Lett., 22 (2012) 2772-2774.
[21] T. Ishikawa, T. Saito, A. Kurosawa, T. Watanabe, S. Maruyama, Y.-i. Ichikawa, R. Yamada, H. Okuzawa, H. Sato, K. Ueno, Chem. Pharm. Bull., 59 (2011) 472-475.
[22] G.M. Cragg, P.G. Grothaus, D.J. Newman, Chem. Rev., 109 (2009) 3012-3043.
[23] K.W. Wellington, RSC Adv., 5 (2015) 20309-20338.
[24] W.H. Choi, J. Ahn, C.H. Jung, Y.J. Jang, T.Y. Ha, Diabetes, 65 (2016) 2490-2501.
[25] X. Liang, Q. Wu, S. Luan, Z. Yin, C. He, L. Yin, Y. Zou, Z. Yuan, L. Li, X. Song, M. He, C. Lv, W. Zhang, Eur. J. Med. Chem., 171 (2019) 129-168.
[26] H. Celik, E. Arinc, J. Pharm. Pharm. Sci., 11 (2008) 68-82.
[27] J. Segura-Aguilar, D. Metodiewa, C.J. Welch, Biochim. Biophys. Acta, Gen. Subj., 1381 (1998) 1-6.
[28] D. Schweinfurth, H.S. Das, F. Weisser, D. Bubrin, B. Sarkar, Inorg. Chem., 50 (2011) 1150-1159.
[29] D. Schweinfurth, M.M. Khusniyarov, D. Bubrin, S. Hohloch, C.-Y. Su, B. Sarkar, Inorg. Chem., 52 (2013) 10332-10339.
[30] H.S. Das, D. Schweinfurth, J. Fiedler, M.M. Khusniyarov, S.M. Mobin, B. Sarkar, Chem. - Eur. J., 20 (2014) 4334-4346.
[31] M.A. Ansari, A. Mandal, A. Paretzki, K. Beyer, W. Kaim, G.K. Lahiri, Inorg. Chem., 55 (2016) 12357-12365.
[32] A. Das, D. Das, T. Kundu, G.K. Lahiri, J. Chem. Sci., 124 (2012) 1181-1189.
[33] N. Deibel, D. Schweinfurth, S. Hohloch, M. Delor, I.V. Sazanovich, M. Towrie, J.A. Weinstein, B. Sarkar, Inorg. Chem., 53 (2014) 1021-1031.
[34] L. Biancalana, L.K. Batchelor, T. Funaioli, S. Zacchini, M. Bortoluzzi, G. Pampaloni, P.J. Dyson, F. Marchetti, Inorg. Chem., 57 (2018) 6669-6685.
[35] R. McCall, M. Miles, P. Lascuna, B. Burney, Z. Patel, K.J. Sidoran, V. Sittaramane, J. Kocerha, D.A. Grossie, J.L. Sessler, K. Arumugam, J.F. Arambula, Chem. Sci., 8 (2017) 5918-5929.
[36] P. Starha, Z. Travnicek, Coord. Chem. Rev., 395 (2019) 130-145.
[37] R.G. Kenny, C.J. Marmion, Chem. Rev., 119 (2019) 1058-1137.
[38] S. Thota, D.A. Rodrigues, D.C. Crans, E.J. Barreiro, J. Med. Chem., 61 (2018) 5805-5821.

[39] S.M. Meier-Menches, C. Gerner, W. Berger, C.G. Hartinger, B.K. Keppler, Chem. Soc. Rev., 47 (2018) 909-928.
[40] M. Hanif, C.G. Hartinger, Future Med. Chem., 10 (2018) 615-617.
[41] J.W. Lown, S.-K. Sim, K.C. Majumdar, R.-Y. Chang, Biochem. Biophys. Res. Commun., 76 (1977) 705-710.
[42] P. Vaupel, F. Kallinowski, P. Okunieff, Cancer Res., 49 (1989) 6449-6465.
[43] D. Hanahan, R.A. Weinberg, Cell, 100 (2000) 57-70.
[44] B.A. Teicher, Cancer and Metastasis Rev., 13 (1994) 139-168.
[45] D.D. Perrin, W.L.F. Armarego, Purification of Laboratory Chemicals. 3rd Ed, 1988.
[46] M.A. Bennett, T.N. Huang, T.W. Matheson, A.K. Smith, Inorganic Syntheses, 21 (1982) 74-78.
[47] J. Catalan, F. Fabero, M. Soledad Guijarro, R.M. Claramunt, M.D. Santa Maria, M.d.l.C. Foces-Foces, F. Hernandez Cano, J. Elguero, R. Sastre, J. Am. Chem. Soc., 112 (1990) 747-759.
[48] G.M. Sheldrick, Acta Crystallogr., Sect. A: Found. Crystallogr., 64 (2008) 112-122.
[49] O.V. Dolomanov, L.J. Bourhis, R.J. Gildea, J.A.K. Howard, H. Puschmann, J. Appl. Crystallogr., 42 (2009) 339-341.
[50] S. Qanungo, M. Wang, A.-L. Nieminen, J. Biol. Chem., 279 (2004) 50455-50464.
[51] K.M. Rouschop, L.J. Dubois, T.G. Keulers, T. van den Beucken, P. Lambin, J. Bussink, A.J. van der Kogel, M. Koritzinsky, B.G. Wouters, Proc. Natl. Acad. Sci., 110 (2013) 4622-4627.
[52] M. Rivlin, U. Eliav, G. Navon, J. Phys. Chem. B, 119 (2015) 4479-4487.
[53] J.P. Lewicki, C.A. Fox, M.A. Worsley, Polymer, 69 (2015) 45-51.
[54] X. Dai, Z.-F. Du, L.-H. Wang, J.-Y. Miao, B.-X. Zhao, Anal. Chim. Acta, 922 (2016) 64-70.
[55] Y. Song, B.A. Wagner, J.R. Witmer, H.-J. Lehmier, G.R. Buettner, Proc. Natl. Acad. Sci., 106 (2009) 9725-9730.
[56] J.L. Bolton, T. Dunlap, Chem. Res. Toxicol., 30 (2017) 13-37.
[57] J.M. Brown, A.J. Giaccia, Cancer res., 58 (1998) 1408-1416.
[58] C. CarlosMenéndez, Medicinal Chemistry of Anticancer Drugs, (2008) 351-385.
[59] N. Watanabe, D.A. Dickinson, R.-M. Liu, H.J. Forman, Methods in Enzymol., 378 (2004) 319-340.
[60] N. Watanabe, H.J. Forman, Arch. Biochem. Biophys., 411 (2003) 145-157.
[61] A.P. Garner, M.J.I. Paine, I. Rodriguez-Crespo, E.C. Chinje, P.O. De Montellano, I.J. Stratford, D.G. Tew, C.R. Wolf, Cancer Res., 59 (1999) 1929-1934.
[62] C. Lind, E. Cadenas, P. Hochstein, L. Ernster, Methods in Enzymol., 186 (1990) 287-301.

Graphical Abstract:

A 1,4 quinone functionalized bis(3,5-dimethylpyazole) ligand complexed with Ru^{II}-*p*-cymene to form a stable complex. The quinone ligand is reduced during metal complexation in methanol to hydroquinone while oxidizing the methanol to formaldehyde. The quinone ligand displays quasi-reversible redox activity, activation under hypoxia and disrupts cellular redox balance by oxidizing NADH, whereas the complexation with Ru^{II} deactivated the redox capability and cytotoxicity due to reduction to hydroquinone.

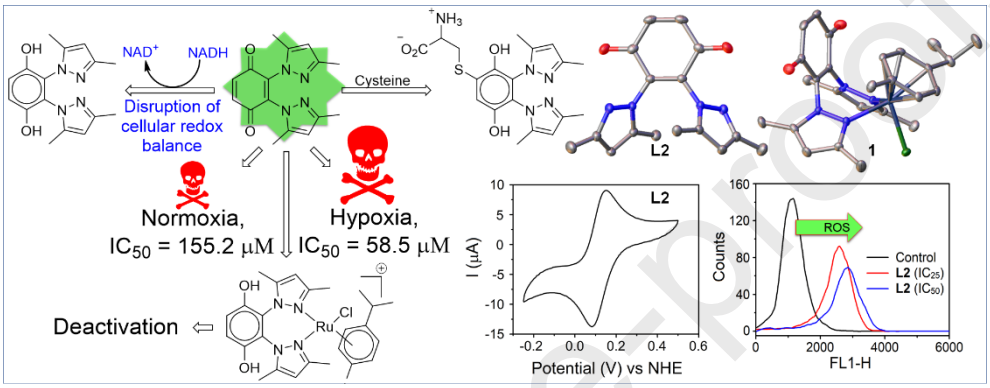

Graphical Abstract:

A 1,4 quinone functionalized bis(3,5-dimethylpyazole) ligand complexed with Ru^{II}-*p*-cymene to form a stable complex. The quinone ligand is reduced during metal complexation in methanol to hydroquinone while oxidizing the methanol to formaldehyde. The quinone ligand displays quasi-reversible redox activity, activation under hypoxia and disrupts cellular redox balance by oxidizing NADH, whereas the complexation with Ru^{II} deactivated the redox capability and cytotoxicity due to reduction to hydroquinone.

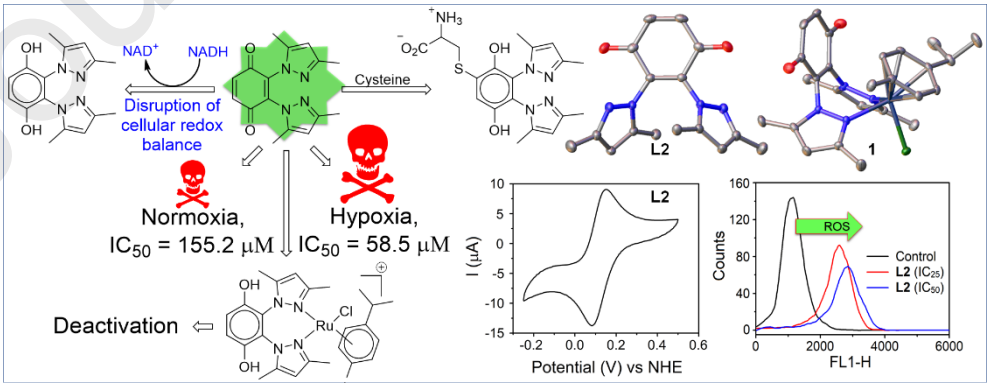

Highlights

- A 1,4-quinone based bis(pyrazole) compound showed ca. 3-fold activation in hypoxia.
- Complexation with Ru^{II} *p*-cym rendered stable metal complex but inactive.
- Methanol reduces the quinone to hydroquinone while oxidizing itself to formaldehyde
- The redox active quinone oxidises NADH to NAD^+ and generates ROS.
- Deactivation observed with cellular thiols

Declaration of interests

☒ The authors declare that they have no known competing financial interests or personal relationships that could have appeared to influence the work reported in this paper.

☐The authors declare the following financial interests/personal relationships which may be considered as potential competing interests:

Kallol purkait

Arindam Mukherjee